

RESEARCH ARTICLE SUMMARY

DEVELOPMENTAL BIOLOGY

Generation of ovarian follicles from mouse pluripotent stem cells

Takashi Yoshino, Takahiro Suzuki, Go Nagamatsu, Haruka Yabukami, Mika Ikegaya, Mami Kishima, Haruka Kita, Takuya Imamura, Kinichi Nakashima, Ryuichi Nishinakamura, Makoto Tachibana, Miki Inoue, Yuichi Shima, Ken-ichirou Morohashi, Katsuhiko Hayashi*

INTRODUCTION: Germ cells develop in a specific environment in the reproductive organs. Throughout oogenesis, oocytes are encapsulated by somatic cells in follicle structures that provide numerous signals and components essential for key events in oocyte development, such as meiosis and growth. The interaction between the oocyte and the somatic follicular cells is regulated in a stage-dependent manner. Recently, in vitro gametogenesis, reconstitution of germ cell development in culture using pluripotent stem cells, has been developed in mammalian species, including mice and humans. In mice, functional oocytes can be produced from pluripotent stem cell-derived primordial germ cell-like cells (PGCLCs) by reaggregation with embryonic ovarian somatic cells at embryonic day 12.5. Therefore, in vitro gametogenesis is expected to be an innovative means of producing a robust number of oocytes in culture. This should be particularly useful for application to humans and endangered animals. However, the in vitro reconstitution of germ cell development is highly dependent on the somatic cell environment provided by embryonic ovarian tissue, which is difficult to obtain from mammalian species. Here, we provide a model system that reconstitutes the ovarian somatic cell environment using mouse pluripotent stem cells.

RATIONALE: During mouse development, the embryonic ovaries originate from the nascent mesoderm, followed by the intermediate mesoderm and coelomic epithelium at the genital ridge region. For the formation of embryonic ovarian somatic cells from mouse pluripotent stem cells, appropriate signals need to be provided in culture to mimic those embryonic events. Using mouse embryonic stem cells (mESCs) harboring reporter constructs that monitor the expression of key genes for each step, we set out to explore culture conditions for the recreation of the differentiation process. Faithful gene expression and functionality should be conferred in induced embryonic ovarian somatic cells under the appropriate conditions. The functionality of the induced cells should be verified by the ability to support the generation of functional oocytes capable of fertilization and subsequent development.

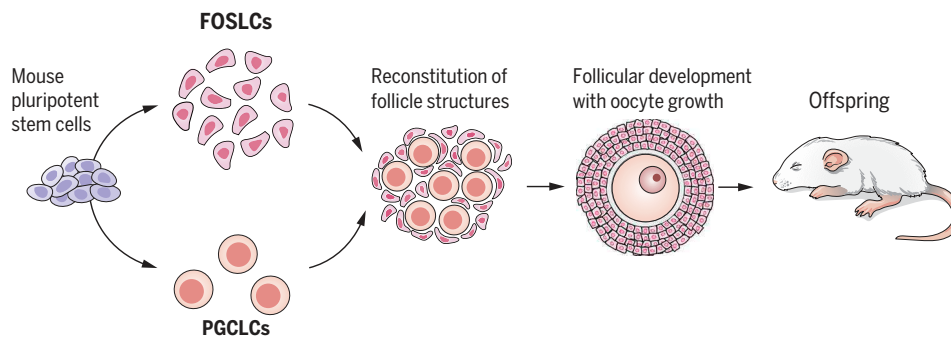
RESULTS: Based on reporter gene expression, we determined a series of culture conditions that recreate the differentiation process from pluripotent cells to gonadal somatic cells in a stepwise manner. Under these conditions, mESCs differentiated into fetal ovarian somatic cell-like cells (FOSLCs) expressing *Nr5a1*, a representative marker gene of gonadal soma-

tic cells, through the nascent mesoderm, intermediate mesoderm, and coelomic epithelium states. FOSLCs exhibited a transcriptional profile and cellular composition similar to those in embryonic ovarian somatic cells at embryonic day 12.5. When FOSLCs were aggregated with PGCLCs derived from mESCs, the PGCLCs entered meiosis, and subsequent oocyte growth accompanied the development of FOSLC-derived follicles in culture. PGCLC-derived oocytes developing in the FOSLC-derived follicles were capable of fertilization and developed to live offspring. These results demonstrate the reconstitution of functional follicle structures that are fully capable of supporting oocyte production.

CONCLUSION: Our results demonstrate that functional gonadal somatic cells can be induced from mESCs through a faithful differentiation process in culture. The generated material may serve as a useful source to replace embryonic ovarian tissue for in vitro gametogenesis. Furthermore, this system contributes to a better understanding of gonadal somatic cell differentiation and the interactions between oocytes and follicular somatic cells. Because it does not require embryonic gonads, the methodology opens the possibility for application in other mammalian species with fewer ethical and technical concerns. This system will accelerate our understanding of gonadal development and provide an alternative source of gametes for research and reproduction. ■

The list of author affiliations is available in the full article online.
*Corresponding author. Email: hayashik@hgs.med.kyushu-u.ac.jp
Cite this article as T. Yoshino et al., *Science* 373, eabe0237 (2021). DOI: 10.1126/science.abe0237

S READ THE FULL ARTICLE AT
<https://doi.org/10.1126/science.abe0237>



Reconstitution of follicle structures, including oocytes, entirely from mouse pluripotent stem cells. Illustrations on the left show a schematic overview of reconstitution of both FOSLCs and PGCLCs from mESCs. Oocytes in the reconstituted environment gave rise to offspring after fertilization. The right image represents fully grown cumulus-oocyte complexes derived from FOSLCs (red) and PGCLCs (blue).

RESEARCH ARTICLE

DEVELOPMENTAL BIOLOGY

Generation of ovarian follicles from mouse pluripotent stem cells

Takashi Yoshino¹, Takahiro Suzuki^{2,3}, Go Nagamatsu¹, Haruka Yabukami², Mika Ikegaya², Mami Kishima², Haruka Kita¹, Takuya Imamura^{1,4}, Kinichi Nakashima¹, Ryuichi Nishinakamura⁵, Makoto Tachibana⁶, Miki Inoue⁷, Yuichi Shima^{7,8,9}, Ken-ichirou Morohashi^{7,8}, Katsuhiko Hayashi^{1*}

Oocytes mature in a specialized fluid-filled sac, the ovarian follicle, which provides signals needed for meiosis and germ cell growth. Methods have been developed to generate functional oocytes from pluripotent stem cell–derived primordial germ cell–like cells (PGCLCs) when placed in culture with embryonic ovarian somatic cells. In this study, we developed culture conditions to recreate the stepwise differentiation process from pluripotent cells to fetal ovarian somatic cell–like cells (FOSLCs). When FOSLCs were aggregated with PGCLCs derived from mouse embryonic stem cells, the PGCLCs entered meiosis to generate functional oocytes capable of fertilization and development to live offspring. Generating functional mouse oocytes in a reconstituted ovarian environment provides a method for in vitro oocyte production and follicle generation for a better understanding of mammalian reproduction.

In mammalian species, oocytes are grown in the ovarian follicles for a long period of time to acquire competence of fertilization. In mice, the interaction of oocytes with surrounding somatic cells commences at embryonic day (E) 10, when the primordial germ cells (PGCs) migrate into the two genital ridges. Somatic cells in the genital ridge provide signal(s) for the proliferation of PGCs while proliferating themselves to form a pair of gonads. Upon sex determination at around E12, female gonadal somatic cells start to differentiate into granulosa cells and interstitial cells, which eventually form ovarian follicle structures (1). After puberty, primary oocytes begin to grow to mature oocytes, and this process is tightly associated with the development of ovarian follicles that provide the support required for oocyte growth and maturation.

Reconstitution in vitro of the entire process of follicular development would enable a better understanding of oocyte development and robust production of oocytes in culture. Recently, we developed a culture system that produces functional oocytes from mouse pluripotent stem cell–derived PGC-like cells (PGCLCs) by reaggregation with female gonadal somatic cells isolated from E12.5 mouse embryos (2). This system is expected to provide a means of producing a robust number of oocytes in culture and should be particularly useful for application to humans and endangered animals. To enable in vitro generation of mouse follicular development, it is also necessary to develop a culture system that allows the induction of functional female gonadal somatic cells from mouse pluripotent stem cells. By combining in vitro oocyte and somatic gonadal cells, it might then be possible to generate a functional ovarian follicle for fertilization and embryonic growth.

ESCs differentiate into gonadal somatic cells under defined conditions

During mouse development, the pluripotent epiblast undergoes multiple steps to form the embryonic gonads (fig. S1A). During gastrulation, the pluripotent epiblast undergoes epithelial-to-mesenchyme transition along the primitive streak, followed by bilateral ingress underneath the epiblast layer (Fig. 1A). The distance from the primitive streak is important for cell fate determination during mesoderm development; that is, along with the mediolateral axis, the notochord, the paraxial mesoderm (PM), the intermediate mesoderm (IMM; which includes somatic precursors of the gonads), and the lateral plate mesoderm

(LPM) are formed. As a step toward in vitro reconstitution of the somatic gonad, we determined a culture condition that efficiently induces the IMM from mouse embryonic stem cells (ESCs) by focusing on *T* and *platelet-derived growth factor receptor-α* (*Pdgfra*) expression: *T* is expressed in the nascent mesoderm at the primitive streak and then eventually restricted in the notochord, whereas *Pdgfra* is expressed in a lateral part of the nascent mesoderm that eventually differentiates into the PM, IMM, or LPM (3, 4) (Fig. 1A). For evaluation of the culture conditions, female ESCs harboring *TⁿE^{GFP}-CreERT2/+* [*T*-green fluorescent protein (*T*-GFP)] (5) (fig. S1B) were first differentiated into epiblast-like cells (EpiLCs) (6) and then cultured in a U-bottomed plate with various combinations of BMP4 and a WNT agonist, CHIR99021 (CHIR) (Fig. 1B). *T*-GFP expression was observed in cell aggregations cultured in the presence of BMP4 or CHIR at 2 days of culture (D2) but disappeared at D4 (fig. S2A). Endogenous T protein was also detected in *T*-GFP–positive cells (fig. S2B). Fluorescence-activated cell sorting (FACS) analysis showed that in the presence of BMP4 or CHIR, most of the cells expressed both *T*-GFP and PDGFRA at D2, and then expressed only PDGFRA at D4 (Fig. 1C and fig. S2C), indicating that the nascent mesoderm–like cells were lateralized during the culture period.

Under these conditions, we monitored the expression of *Osr1* and *Foxf1*, which are representative marker genes for IMM and LPM, respectively (7, 8) (Fig. 1D and fig. S1, A and B), by using *Foxf1*-tdTomato/*Osr1*-GFP reporter ESCs (fig. S3A). *Foxf1*-tdTomato was induced by BMP4 in a dose-dependent manner (Fig. 1E and fig. S3, B and C), consistent with evidence that BMP4 lateralizes the mesoderm in vivo (9). *Osr1*-GFP was induced at a high concentration of CHIR with BMP4, but the effect was attenuated by an increased concentration of BMP4 (Fig. 1E and fig. S3, B and C), suggesting a mutually exclusive function of BMP and WNT signaling on the determination of LPM and IMM. Supporting this observation, quantitative polymerase chain reaction (Q-PCR) analysis of the marker gene expression showed that a high concentration of CHIR promoted the expression of the IMM genes but prevented that of the LPM genes (fig. S3D). Under these conditions, the expression of the PM markers *Uncx4* and *Tbx2* remained at a very low level. Based on the enrichment of the *Osr1*-positive/*Foxf1*-negative cell population and transcripts of the IMM marker genes, we fixed the concentrations of BMP4 and CHIR at 1 ng/ml and 14 μM, respectively, for the subsequent culture experiments.

It is known that the mesoderm after gastrulation is anteriorized by retinoic acid (RA) and in contrast posteriorized by fibroblast growth factor (FGF) and Wnt signaling (10–12). In

¹Department of Stem Cell Biology and Medicine, Graduate School of Medical Sciences, Kyushu University, Higashi-ku, Fukuoka 812-8582, Japan. ²Laboratory for Cellular Function Conversion Technology, RIKEN Center for Integrative Medical Sciences, Yokohama, Kanagawa 230-0045, Japan.

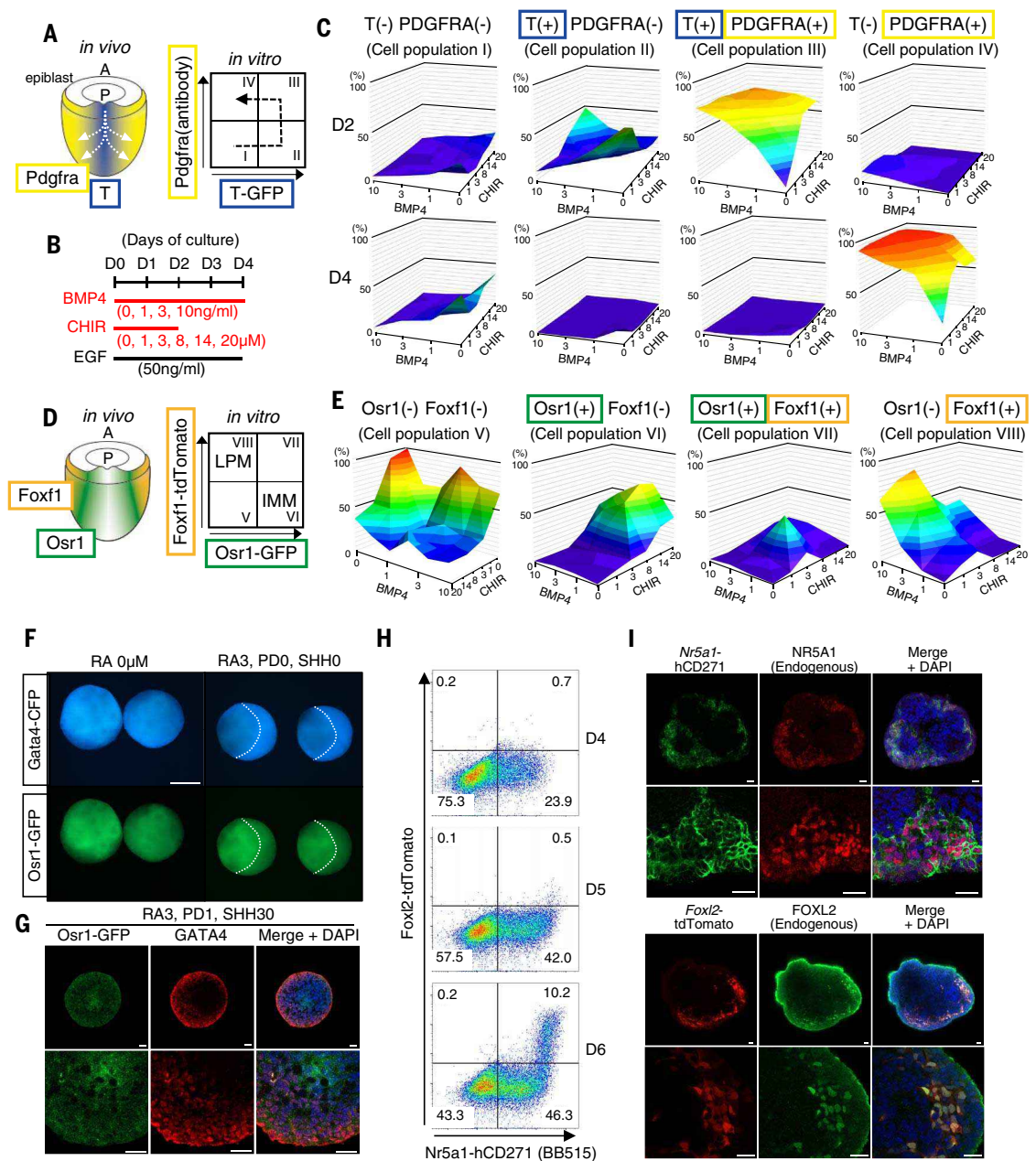
³Functional Genomics, Graduate School of Medical Life Science, Yokohama City University, Yokohama, Kanagawa, 230-0045, Japan. ⁴RNA Biology and Epigenomics Team/LMCP, Program of Biomedical Science, Graduate School of Integrated Sciences for Life, Hiroshima University, Higashi-Hiroshima City, Hiroshima 739-8511, Japan. ⁵Department of Kidney Development, Institute of Molecular Embryology and Genetics, Kumamoto University, Chuo-ku, Kumamoto 860-0811, Japan. ⁶Laboratory of Epigenome Dynamics, Graduate School of Frontier Biosciences, Osaka University, Suita, Osaka 565-0871, Japan. ⁷Department of Molecular Biology, Graduate School of Medical Sciences, Kyushu University, Higashi-ku, Fukuoka City 812-8582, Japan. ⁸Department of Systems Life Sciences, Graduate School of Systems Life Sciences, Kyushu University, Higashi-ku, Fukuoka City 812-8582, Japan. ⁹Department of Anatomy, Kawasaki Medical School, Kurashiki City, 701-0192 Okayama Prefecture, Japan.

*Corresponding author. Email: hayashik@hgs.med.kyushu-u.ac.jp

Fig. 1. Sequential differentiation to the gonadal somatic cell precursor.

(A) Marker genes for monitoring nascent mesoderm differentiation. The left diagram shows embryonic regions expressing *T* (blue) and *Pdgfra* (yellow) in the mesoderm. White arrows indicate the direction of the spreading mesoderm. The right diagram shows an expected sequence of nascent mesodermal differentiation in the FACS analysis. A, anterior; P, posterior.

(B) Culture conditions tested for nascent mesoderm differentiation. D0 corresponds to EpiLCs. **(C)** Summary of FACS analysis of T-GFP and PDGFRA. Graphs show the percentage of each cell population differentiated under various concentrations of BMP4 and CHIR at D2 and D4. The Roman numerals in the parentheses correspond to the cell population shown in (A). The mean percentage in biologically triplicate experiments is shown. **(D)** Marker genes for monitoring intermediate mesoderm differentiation. The diagrams show embryonic regions expressing *Osr1* (green) and *Foxf1* (orange) (left) and an expected FACS pattern representing IMM and LPM (right). **(E)** Summary of the FACS analysis of *Osr1*-GFP and *Foxf1*-tdTomato. Graphs show the percentage of each cell population differentiated under the conditions shown in (B). The mean percentage in biologically triplicate experiments is shown. **(F)** Distinct distribution of the *Gata4*-CFP-positive cell population. The images show cell aggregations at 4 days in the culture with or without 3 μ M RA (RA3). Note that the cultures with RA show mutually exclusive distribution between *Gata4*-CFP-positive and *Osr1*-GFP-positive cells, the border lines of which are indicated by white lines. Scale bars, 200 μ m. **(G)** Expression of *Osr1*-GFP and endogenous GATA4 protein. Shown are the results of immunostaining of *Osr1*-GFP and GATA4 protein and merged images with 4',6'-diamidino-2-



phenylindole (DAPI; blue) in a section of the *Osr1*-GFP ESC aggregate at 4 days in culture with RA3, 1 μ M PD (PD1), and 30 ng/ml SHH (SHH30). Scale bars, 20 μ m. **(H)** Differentiation of *Nr5a1*-hCD271-positive cells. Shown are the FACS profiles of Nr271F2T ESCs cultured for the number of days indicated. The numbers in the plot represent the percentages of each cell population. **(I)** Expression of NR5A1 and FOXL2 in the aggregates. Shown are immunofluorescence images of the reporter and endogenous protein indicated and merged images with DAPI (blue) in a section of the Nr271F2T ESC aggregate cultured at D6. Scale bars, 20 μ m.

addition, Sonic hedgehog (SHH) is involved in specification of the ventromedial coelomic epithelium in chick embryos (13). Therefore, for induction of the anterior ventral IMM, which should contain the precursors of the genital ridge, we tested the effect of RA, the

FGF inhibitor PD0325901 (PD), and SHH by adding each of these reagents at D2 (fig. S4A). To monitor differentiation into the precursors of the genital ridge, we inserted the *enhanced cyan fluorescent protein (ECFP)* gene into the locus of *Gata4*, the earliest functional marker

gene for the genital ridge formation (14), in female *Osr1*-GFP ESCs, thereby producing *Osr1*-GFP/*Gata4*-CFP ESCs (fig. S4B). The addition of RA slightly up-regulated *Gata4*-CFP and down-regulated *Osr1*-GFP, whereas PD or SHH had no obvious impact on their

expression (fig. S4C). Q-PCR reinforced the slight up-regulation of *Gata4*, *Lhx9*, and *Wtl*, functional marker genes for gonadal somatic cell precursors (14–16), in response to RA (fig. S4D). Mutually exclusive distributions of *Gata4*-CFP-positive cells and *Osr1*-GFP-positive cells were observed in the presence of RA (Fig. 1F and fig. S4E). This pattern was confirmed with endogenous GATA4 protein in the *Osr1*-GFP ESC aggregates (Fig. 1G). This exclusive pattern is consistent with that in gonadal somatic cell precursors in vivo (fig. S4F). Despite the subtle effects or lack of effect of PD and SHH on *Gata4*, *Lhx9*, or *Wtl* expression, the addition of these factors resulted in an increased number of *Gata4*-CFP-positive/*Osr1*-GFP-low cells (fig. S4G). Based on these marker gene expressions and on the number of *Gata4*-CFP-positive/*Osr1*-GFP-low cells produced, we fixed the concentrations of RA, PD, and SHH at 3 μ M, 1 μ M and 30 ng/ml, respectively, for the subsequent culture experiments.

Nr5a1 is expressed in all cell lineages in the genital ridge (1, 17), and its expression is coordinated by various transcription factors that are essential for gonadal development, such as GATA4 (14), EMX2 (18), WT1 (15, 16), and LHX9 (15), therefore indicating that *Nr5a1* is the most stringent marker for differentiation into gonadal somatic cells. To monitor *Nr5a1* expression, we derived female ESCs from *Nr5a1*-hCD271 bacterial artificial chromosome transgenic mice (19) (fig. S1B), in which human *CD271* gene is driven by the *Nr5a1* promoter. Using *Nr5a1*-hCD271 ESCs, we inserted the *tdTomato* gene into the *Foxl2* locus, a marker gene for granulosa cells (20), thereby producing *Nr5a1*-hCD271/*Foxl2*-tdTomato (Nr271F2T) ESCs (fig. S5A). When Nr271F2T ESCs were cultured under the conditions described above, *Nr5a1*-hCD271 was detectable in a group of cells at D4 (Fig. 1H). As the culture progressed in the medium containing BMP4 (20 ng/ml) and a low dose of FGF9 (2 ng/ml), the percentage of *Nr5a1*-hCD271-positive cells increased. From D6 onward, *Foxl2*-tdTomato-positive cells appeared (Fig. 1H and fig. S5B). Immunofluorescence analysis confirmed endogenous NR5A1 and FOXL2 expression in the cells expressing the reporter genes (Fig. 1I). In mouse development, the expression of *Foxl2* has been shown to be detectable in the female gonad from E12.5 (21, 22). Given that EpiLCs correspond to E5.75 epiblasts (6), the fact that a total of 6 days after EpiLC differentiation was required for the differentiation of *Foxl2*-tdTomato-positive cells was largely consistent with the time course of development in vivo.

ESC derivatives share similar properties with gonadal somatic cells in vivo

To analyze the cell populations induced, we applied single-cell RNA-sequencing analysis of *Nr5a1*-hCD271-positive cells sorted by

magnetic-activated cell sorting (MACS) (fig. S6A). Comparison of the expression profiles of *Nr5a1*-hCD271-positive cells at D6 with those of cells in the gonads from E10.5 to E14.5 embryos revealed a similar pattern of cell clusters between E11.5 and E14.5 (Fig. 2A). The numbers of clusters 0, 1, 2, 4, and 5 were comparable both in vitro and in vivo, whereas other clusters were fewer in vitro. Based on the expression of marker genes defined by a previous transcriptome study (1), it appears that clusters 0, 1, 2, 4, and 5 include granulosa cell, stromal cell, or early progenitor cell populations, and clusters 3, 6, 7, and 8, which were few in vitro, correspond to germ cell, endothelial cell, erythrocyte, and megakaryocyte populations, respectively (Fig. 2B and fig. S6B). The differentiation of germ cell-like cells was confirmed by evidence that cells expressing *Blimp1*-mVenus (BV), *stella*-CFP (SC), and POU5F1 were sparsely induced under these conditions (fig. S6C). These germ cell-like cells, as well as endothelial cells, erythrocytes, and megakaryocytes, could be induced by BMP4 and WNT signals that promote the differentiation of PGCs and *Flk1*-positive common progenitors of hematopoietic and endothelial cells from ESCs (6, 23). Because *Nr5a1* expression was undetectable in clusters 3, 6, 7, and 8 (fig. S6D), these minor populations might have been the result of insufficient removal by MACS.

To analyze the gonadal somatic cells that directly contribute to the follicle structure, we compared single-cell profiles between *Nr5a1*-hCD271-positive cells at D6 and E12.5 gonadal somatic cells (fig. S6E) because FOXL2 expression was first detectable at those stages in vitro and in vivo, respectively (Fig. 1H) (22). After excluding the germ cell, endothelial cell, and hematopoietic cell populations (fig. S6F), the remaining populations could be reclassified into six clusters, S0 to S5 (Fig. 2C). Cells expressing the granulosa cell marker genes were enriched in clusters S2 and S4, and cells expressing the stromal cell marker genes were enriched mainly in cluster S3 and partially in cluster S0 (fig. S6G). The expressions of some stromal cell marker genes, such as *Wnt5a* and *Tcf21*, were detectable in cells belonging to clusters S1 and S5. In clusters S1 and S5, the expressions of early progenitor marker genes (1) such as *Sox11*, *Ecml*, and *Nr2f1* were detectable, indicating that these clusters contain early progenitors. The close similarity in gene expression between the cluster S0/S3 expressing stromal markers and the cluster S1/S5 expressing early progenitor markers was consistent with the fact that early progenitors and stromal cell progenitors share a similar gene expression profile (1). *Nr5a1* was widely expressed and enriched in clusters S2 and S4 (fig. S6G), consistent with the evidence that *Foxl2*-tdTomato-positive cells appeared from

the *Nr5a1*-hCD271-highly positive cell population (Fig. 1H). Conversely, *Nr5a1* was not detectable in some cells. The heterogeneous level of endogenous NR5A1 protein expression (Fig. 1I) indicates that the expression of *Nr5a1* was highly heterogeneous at the transcript and protein levels. Because of the substantial contribution of the cell cycle state to the gene expression profile (24, 25), we estimated the cell cycle stage in each cell population. This analysis suggested that cluster S5 was actively proliferative and portions of clusters S0 and S3 were also proliferative (Fig. 2D). By contrast, most cells in clusters S2 and S4 were in G₁, consistent with previous findings that cells expressing *Foxl2* arrested their cell cycle through p27 and CDKN1B (22, 26). Genes involved in epithelial cell function and ovarian epithelial cancer, such as *Krt19*, *Upk3b*, and *Itm2a*, were expressed in clusters S1 and S5 (fig. S6H), suggesting that these clusters could include the surface epithelium of the fetal ovary, known to be the source of granulosa cells (26). Based on these observations, we designated clusters S2 and S4 as granulosa cells; clusters S0 and S3 as stromal cell progenitors and stromal cells, respectively; and clusters S1 and S5 as early progenitors (Fig. 2C). The percentage of granulosa cells was smaller in the cell population differentiated in vitro than that in vivo (Fig. 2E). This may have been caused by a delay in granulosa cell differentiation in culture (see below). Comparison of the gene expression in each cluster between the in vivo and in vitro differentiations showed that they were highly similar ($R > 0.96$) (Fig. 2F and fig. S6I). Based on the similar pattern of cell clusters and of gene expression within each cluster, we concluded that the *Nr5a1*-hCD271-positive cell population was similar to the E12.5 gonadal somatic cell population. We thereafter named the *Nr5a1*-hCD271-positive cells fetal ovarian somatic cell-like cells (FOSLCs).

FOSLCs support oocyte development

To evaluate function, FOSLCs were reaggregated with PGCLCs harboring BV and SC reporter genes. Considering that PGCLCs correspond to E9.5 PGCs (6), we sorted FOSLCs at D5 by MACS, which yielded 7640 ± 1670 (\pm SE, $n = 10$ replicates) FOSLCs on average from one aggregation. Because the exact ratio of PGCs to gonadal somatic cells in the nascent genital ridge is difficult to define, following the ratio (5 to 18%) in the E12.5 gonads (27), 5000 PGCLCs harboring the BV and SC reporter genes were reaggregated with 75,000 or 100,000 FOSLCs and then cultured under in vitro differentiation culture (IVDi) conditions (2). Many oocytes were formed in the reaggregates (Fig. 3A), which were thereafter called reconstituted ovaroids (rOvaroids) to distinguish them from the ovaroids containing E12.5 gonadal somatic cells. This oocyte formation relied on FOSLCs or gonadal somatic cells because

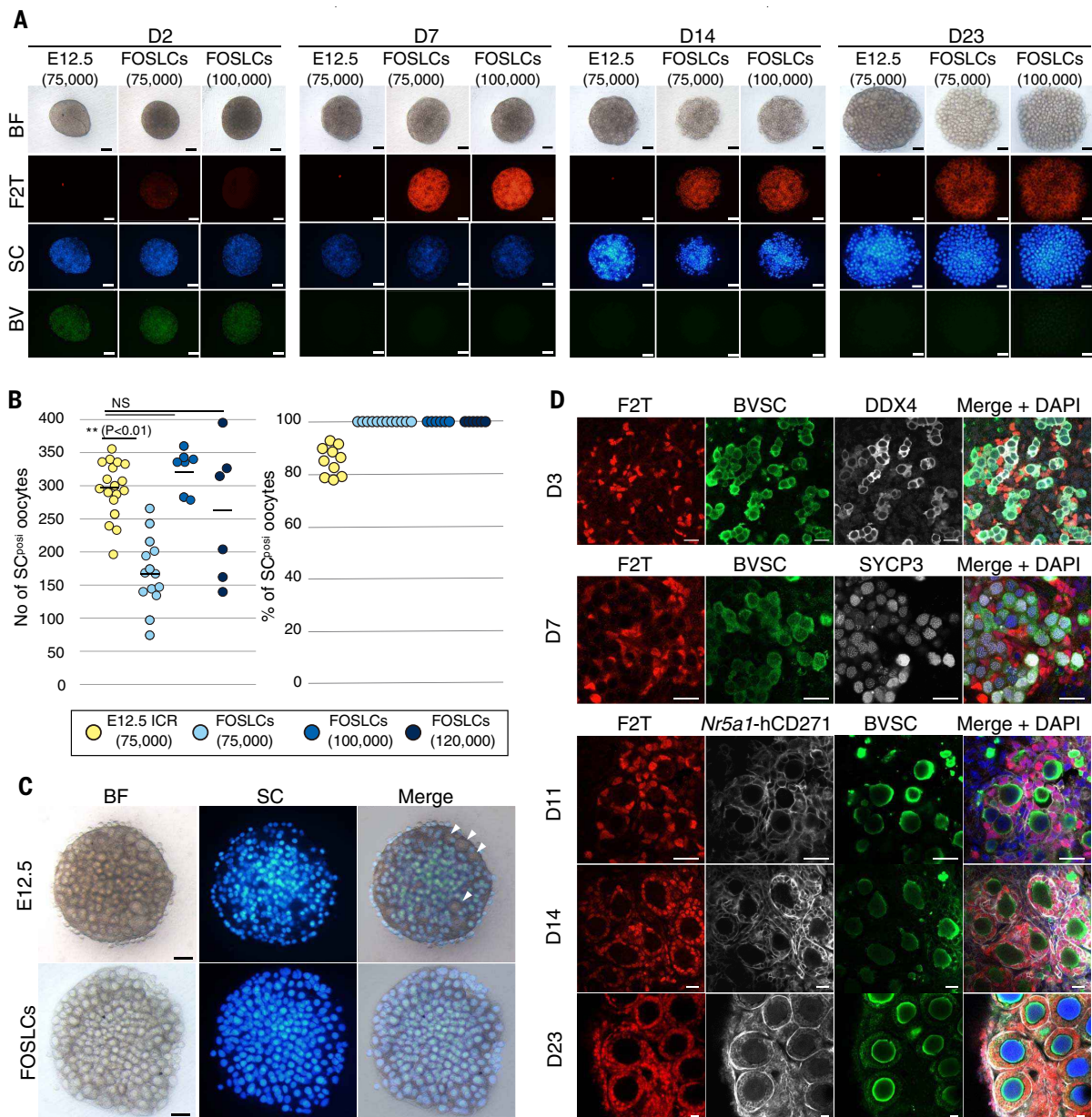


Fig. 3. Oogenesis in the culture system using FOSLCs. (A) IVDi culture using FOSLCs. Images show PGCLCs reaggregated with E12.5 gonadal somatic cells or FOSLCs cultured for the number of days indicated. The numbers in parentheses are the numbers of E12.5 gonadal somatic cells or FOSLCs cells used. BF, bright field. Scale bars, 200 μ m. **(B)** Summary of oocytes yielded in IVDi culture. Shown are the number of oocytes (left) and the percentage of SC-positive oocytes (right) in the ovarioid or the rOvarioid at day 23 of culture. The numbers of oocytes were determined by counting SC-positive cells in the image. The values were obtained

from at least three biologically independent experiments. The bars in the graph indicate the mean value. *P* values relative to the control were determined using Student's *t* test. **(C)** Complete elimination of endogenous oocytes in an rOvarioid. BF and fluorescence images show an ovarioid using 75,000 E12.5 gonadal somatic cells and an rOvarioid using 100,000 FOSLCs. SC-negative oocytes were observed in the ovarioid (arrowheads). Scale bars, 200 μ m. **(D)** Immunofluorescence analysis of oocyte development in the rOvarioid. Shown are immunofluorescence images of the antigens indicated and merged images with DAPI (blue). Scale bars, 20 μ m.

it became comparable in rOvarioids with 100,000 FOSLCs (Fig. 3B). The productivity was not improved in rOvarioids with 120,000 FOSLCs. This inferior potential of FOSLCs to become embryonic gonadal somatic cells was largely reproducible under the same genetic background; the number of oocytes in rOvarioids with FOSLCs derived from C57BL/6J ESCs was reduced to 67.4% of that in ovarioids with

E12.5 C57BL/6J gonadal somatic cells (fig. S7, B and C). All oocytes in the rOvarioids were SC positive, in contrast to ovarioids, which contained SC-negative oocytes derived from residual PGCs mingled in the E12.5 gonadal somatic cells despite depletion by antibodies specific for PGCs (Fig. 3, B and C). This result demonstrated that the rOvarioid completely eliminated contamination of residual oocytes,

which is important to ensure the origin of oocytes. In addition, the uniform SC expression also rules out the possibility that cells expressing germ cell markers found in the FOSLCs contribute to oocytes in the rOvarioid.

We next verified the differentiation process in rOvarioids using immunofluorescence analyses. At D3, *Foxl2*-tdTomato-positive cells started to surround PGCLCs that appeared to

proliferate to form germ cell cysts with expression of DDX4, a later germ cell marker (Fig. 3D and fig. S8, A and B). At D7, PGCLCs entered meiosis, thereby differentiating oocytes, with typical alignments of the SYCP3 protein. Individual follicle structures with *Foxl2*-tdTomato-positive cells were formed by D11. At this stage, oocytes degrading in the rOvaroids were frequently observed (fig. S8C), consistent with our previous report that oocyte loss accompanied with apoptosis was observed in ovaroids at D11 (28). As the culture progressed, *Foxl2*-tdTomato-positive granulosa-like cells became stratified and *Nr5a1*-hCD271 expression was more prominent in the cells surrounding the follicle structure than in *Foxl2*-tdTomato-positive granulosa-like cells (Fig. 3D and fig. S8B). This is consistent with evidence in vivo that NR5A1 becomes prominent in theca and stromal cells but is down-regulated in granulosa cells during follicle development (29, 30). At D23, the formation of secondary follicle structures composed of SC-positive oocytes with a multilayer of *Foxl2*-tdTomato-positive granulosa-like cells and the far surrounding *Nr5a1*-hCD271-positive theca-like cells was observed.

To investigate changes in the competence of FOSLCs during differentiation, PGCLCs were reaggregated with FOSLCs at day 4, 5, 6, 7, or 8 of culture. FACS analysis during the differentiation period showed an increase in the percentage of *Foxl2*-tdTomato-positive cells after D6 (fig. S9A). The analysis also showed that the *Nr5a1*-hCD271-positive/PDGFR α -negative cells, which was the major population at D5, differentiated into either *Nr5a1*-hCD271-highly positive/PDGFR α -negative cells or *Nr5a1*-hCD271-positive/PDGFR α -positive cells, which, based on the marker gene expression (fig. S6G), are granulosa and stromal cells, respectively. When aggregated with PGCLCs, FOSLCs at D5 and D6 showed a high potential for supporting oogenesis (fig. S9B), suggesting that FOSLCs interact with PGCLCs in a timely fashion. Based on marker gene expression, FOSLCs at D6 can be divided into three subpopulations: *Foxl2*-tdTomato-positive (F2T⁺) cells, *Foxl2*-tdTomato-negative and PDGFR α -positive (F2T-P⁺) cells, and *Foxl2*-tdTomato-negative and PDGFR α -negative (F2T-P⁻) cells (fig. S10A). Genes for granulosa cells were enriched, as expected, in the F2T⁺ cell population (fig. S10B). Although the F2T-P⁺ and F2T-P⁻ cell populations could not be clearly distinguished, genes for stromal-stromal progenitor cells were slightly enriched in the F2T-P⁺ cell population. When aggregated with PGCLCs, F2T-P⁺ and F2T-P⁻ cells restored *Foxl2*-tdTomato expression by D7 and formed a number of follicle structures, whereas the F2T⁺ cell population formed a significantly smaller number of follicle structures (fig. S10, C and D). These results indicate that the F2T-P⁺ and F2T-P⁻ populations contain cells that still have

the plasticity to differentiate into granulosa cells and the capability to form follicle structures. This plasticity is consistent with the observation that the granulosa cell population continuously increased after D6 (fig. S9A). Given that the percentage of granulosa cells was smaller in the cell population differentiated in vitro at D6 than in that in vivo (Fig. 2E), the differentiation of granulosa cells may be delayed in the culture system because of an unknown condition that was not fully recapitulated in culture.

Oocytes acquire developmental competence in the culture system using FOSLCs

Developmental competence of FOSLCs was further validated by in vitro growth culture (IVG), in which secondary follicles grow up to a stage equivalent to pre-ovulatory follicles (2). In the IVG culture, FOSLC-derived granulosa cells proliferated and formed cumulus-oocyte complexes (COCs) by D12 with the formation of transzonal projections (TZPs), which are essential for juxtacrine interaction to support oocyte growth (31) (Fig. 4, A and B). Under in vitro maturation culture (IVM) conditions (2), FOSLC-derived cumulus cells were expanded, as is typically observed in maturation of cumulus cells (Fig. 4C). These cumulus cells were readily dispersed by treatment with hyaluronidase, and 28.4% (33/116) of the isolated oocytes proceeded to the MII stage with extrusion of the first polar body (Fig. 4D and table S1). This developmental rate to the MII stage in rOvaroids was comparable to that derived from reaggregates using E12.5 gonadal somatic cells in our previous report (2) (28.9%, 923/3198; $P = 0.994$ by Pearson's chi-square test).

We then used mature COCs from rOvaroids for in vitro fertilization (IVF) using wild-type sperm from ICR mice. In IVF followed by in vitro culture, oocytes were fertilized, and 30.2% (301/996) of oocytes used in the IVF became two-cell embryos (Fig. 4D and table S2). Then, 25.8% (24/93) of the two-cell embryos developed to blastocysts (Fig. 4D and table S3). This developmental rate from two-cell embryos to blastocysts was comparable to that observed in embryos derived from reaggregates using E12.5 gonadal somatic cells in our previous report (2) (31.8%, 44/138; $P = 0.397$ by Pearson's chi-square test). When the two-cell embryos were transferred into pseudopregnant females, 5.2% (11/212) of the embryos gave rise to offspring and all of them developed to adult mice (Fig. 4, E and F, and table S4). This developmental rate to offspring was comparable to that derived from reaggregates using E12.5 gonadal somatic cells in our previous report (2) (3.5%, 11/316; $P = 0.459$ by Pearson's chi-square test). All offspring had dark eyes and some of them had the *BV* or *SC* reporter gene (Fig. 4, F and G), consistent with the fact that the ESCs used were derived from the F₁ blastocyst (129X1/Svj \times C57Bl/6J) and

were heterozygous for the reporter genes. Two independent pairs of these mice produced 10 and 14 pups by their intercrosses (Fig. 4H), and 17 out of 21 pups tested had the *BV* and/or *SC* reporter genes (Fig. 4I), demonstrating their fertility in both males and females. These results demonstrated that mouse oocytes produced in the ovarian environment entirely reconstituted by pluripotent stem cells acquired the competence for fertilization followed by development to term.

Applicability of FOSLCs

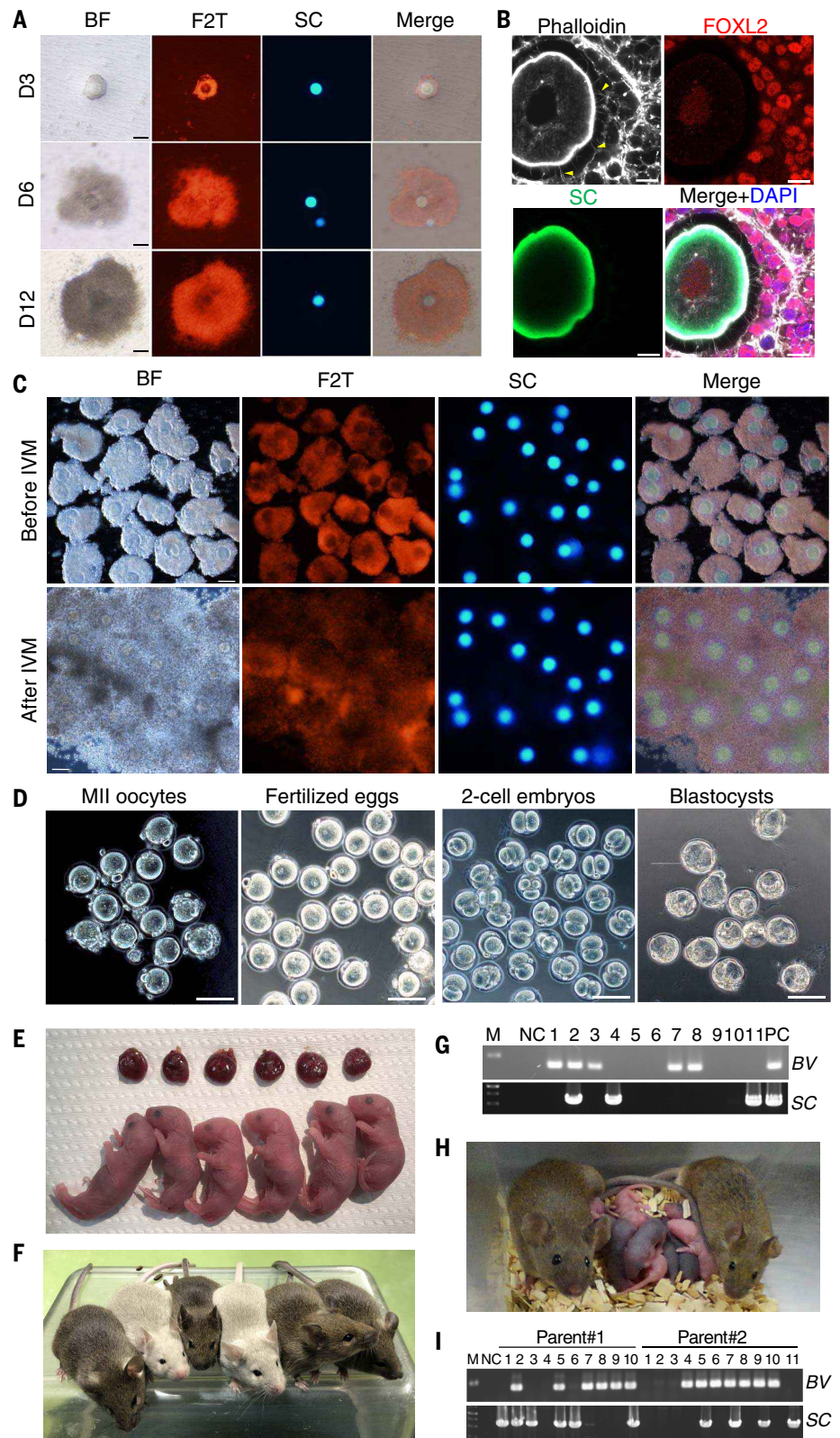
In our system, purification of FOSLCs is greatly dependent on the *Nr5a1*-reporter construct. This requirement may compromise the applicability of this system because of the time-consuming and laborious processes needed for the production of the reporter cell line. Therefore, we tried to provide an rOvaroid system without the need for a reporter gene. The main reason for requiring a reporter system was the appearance of massively proliferative cells, which severely disturbed oogenesis, in reaggregations without purification of FOSLCs (fig. S11A). Because such proliferative cells were observed in the aggregates containing undifferentiated cells (32, 33), they were likely to lie in the *Nr5a1*-hCD271-negative cell population. Indeed, the proliferative cells almost exclusively appeared in aggregates with *Nr5a1*-hCD271-negative cells (fig. S11B). Therefore, we tried to remove the source of the proliferative cells by using antibodies against endogenous SSEA1 and CD31 because pluripotent stem cells express SSEA1 and CD31 (34), and these markers were indeed expressed in a small subset of *Nr5a1*-hCD271-negative cells (fig. S11C). rOvaroids with the cell fraction in the flow-through after the depletion with SSEA1 and CD31 antibodies yielded a number of follicle structures without a proliferative cell clump (fig. S11, D and E). These results demonstrate that the depletion method eliminates the origin of proliferative cells, and therefore a reporter construct is dispensable for the rOvaroid system, which would help to expand the applicability of this system to production of oocytes from pluripotent stem cells without embryonic tissues.

Outlook

Here, we have established a culture system that reconstitutes functional ovarian follicles, including oocytes, from pluripotent stem cells. This system provides several insights for enhancing our understanding and reconstitution of oogenesis. First, this culture system would be an efficient tool for understanding the molecular mechanisms underlying the differentiation of gonadal somatic cells. Second, it enables us to address the interaction between PGCs and/or oocytes and gonadal somatic cells. Because this system can separately

Fig. 4. Full-term development of embryos derived from rOvaroids.

(A) IVG culture using FOSLCs. Shown are BF and fluorescence images of reconstituted follicles cultured for the number of days indicated after isolation of individual follicles. Abbreviations are as shown in Fig. 3A. Scale bars, 100 μ m. **(B)** Formation of TZPs. Shown are fluorescence images of a COC stained with phalloidin and the antibodies indicated. TZPs were formed between the granulosa cells and the oocyte (arrowheads). Scale bars, 10 μ m. **(C)** IVM culture using FOSLCs. Shown are BF and fluorescence images of COCs before or after IVM. Note that cumulus cells after IVM were expanded. Scale bars, 100 μ m. **(D)** MII oocytes and preimplantation embryos derived from rOvaroids. Scale bars, 100 μ m. **(E)** Newborn pups derived from rOvaroids. Shown are pups with placentae obtained by transferring two-cell embryos. **(F)** Adult mice from the newborn pups 4 weeks after birth. **(G)** Detection of reporter genes in the mice derived from rOvaroids. Shown are gel electrophoresis of PCR products to detect BV or SC in the genome. **(H)** Fertility of the adult mice obtained. Shown are pups derived from the intercrossing of the adult mice derived from rOvaroids. **(I)** Detection of reporter genes in the pups derived from two pairs of the adult mice. Shown are the results of gel electrophoresis of PCR products to detect BV or SC in the genome.



Downloaded from <http://science.sciencemag.org/> on July 21, 2021

produce FOSLCs and PGCLCs, which are equivalent to nascent gonadal somatic cells and premeiotic PGCs (6), respectively, it becomes possible to investigate the first and subsequent

interactions between these cell types. Last, this culture system opens the possibility of applying in vitro gametogenesis to other mammalian species. The scarcity of embryonic gonadal

somatic cells is an obstacle to the application of in vitro gametogenesis to mammalian species other than mice. FOSLCs could be an optimal substitute for embryonic tissue because

they have full potency to support oogenesis. For these reasons, this system will be a useful tool for solving key issues in reproductive biology and regenerative medicine.

Methods summary

For FOSLC induction, *Nr5A1*-hCD271 reporter ESCs were differentiated into EpiLCs with activin A and basic FGF. The EpiLCs were cultured in a low-cell-binding, U-bottomed, 96-well plate with 14 μ M CHIR99021, 1 ng/ml BMP4, and 50 ng/ml epidermal growth factor (EGF) for 2 days; then with 3 μ M RA, 30 ng/ml Shh, 1 μ M PD0325901, 50 ng/ml EGF, and 1 ng/ml BMP4 for another 2 days; and then with 20 ng/ml BMP4 and 2 ng/ml FGF9 for another 1 or 2 days. *Nr5A1*-hCD271-positive FOSLCs were purified by MACS using anti-hCD271 antibody conjugated with microbeads and an MS column. For the production of MII oocytes in rOvarioids, FOSLCs were re-aggregated with PGCLCs in a low-cell-binding, U-bottomed, 96-well plate. The rOvarioids were placed on Transwell-COL membranes and then cultured under IVDI conditions for 21 days. Individual follicles were isolated from the rOvarioids and then cultured under IVG conditions for 12 days. Cumulus-oocyte complexes were collected by a fine glass capillary and then cultured under IVM conditions for 16 hours. MII oocytes obtained after IVM culture were subjected to IVF.

REFERENCES AND NOTES

1. Stévant *et al.*, Dissecting cell lineage specification and sex fate determination in gonadal somatic cells using single-cell transcriptomics. *Cell Rep.* **26**, 3272–3283.e3 (2019). doi: [10.1016/j.celrep.2019.02.069](https://doi.org/10.1016/j.celrep.2019.02.069); pmid: 30893600
2. Hikabe *et al.*, Reconstitution in vitro of the entire cycle of the mouse female germ line. *Nature* **539**, 299–303 (2016). doi: [10.1038/nature20104](https://doi.org/10.1038/nature20104); pmid: 27750280
3. D. G. Wilkinson, S. Bhatt, B. G. Herrmann, Expression pattern of the mouse T gene and its role in mesoderm formation. *Nature* **343**, 657–659 (1990). doi: [10.1038/343657a0](https://doi.org/10.1038/343657a0); pmid: 1689462
4. Kataoka *et al.*, Expressions of PDGF receptor alpha, c-Kit and Flk1 genes clustering in mouse chromosome 5 define distinct subsets of nascent mesodermal cells. *Dev. Growth Differ.* **39**, 729–740 (1997). doi: [10.1046/j.1440-169X.1997.t015-00009.x](https://doi.org/10.1046/j.1440-169X.1997.t015-00009.x); pmid: 9493833
5. Imuta, H. Kiyonari, C. W. Jang, R. R. Behringer, H. Sasaki, Generation of knock-in mice that express nuclear enhanced green fluorescent protein and tamoxifen-inducible Cre recombinase in the notochord from Foxa2 and T loci. *Genesis* **51**, 210–218 (2013). doi: [10.1002/dvg.22376](https://doi.org/10.1002/dvg.22376); pmid: 23359409
6. Hayashi, H. Ohta, K. Kurimoto, S. Aramaki, M. Saitou, Reconstitution of the mouse germ cell specification pathway in culture by pluripotent stem cells. *Cell* **146**, 519–532 (2011). doi: [10.1016/j.cell.2011.06.052](https://doi.org/10.1016/j.cell.2011.06.052); pmid: 21820164
7. Mahlapuu, M. Ormestad, S. Enerbäck, P. Carlsson, The forkhead transcription factor Foxl1 is required for differentiation of extra-embryonic and lateral plate mesoderm. *Development* **128**, 155–166 (2001). doi: [10.1242/dev.128.2.155](https://doi.org/10.1242/dev.128.2.155); pmid: 11124112
8. J. W. Mugford, P. Sipilä, J. A. McMahon, A. P. McMahon, Osr1 expression demarcates a multi-potent population of intermediate mesoderm that undergoes progressive restriction to an Osr1-dependent nephron progenitor compartment within the mammalian kidney. *Dev. Biol.* **324**, 88–98 (2008). doi: [10.1016/j.ydbio.2008.09.010](https://doi.org/10.1016/j.ydbio.2008.09.010); pmid: 18835385
9. A. Rojas *et al.*, Gata4 expression in lateral mesoderm is downstream of BMP4 and is activated directly by Forkhead and GATA transcription factors through a distal enhancer element. *Development* **132**, 3405–3417 (2005). doi: [10.1242/dev.01913](https://doi.org/10.1242/dev.01913); pmid: 15987774
10. S. Takada *et al.*, Wnt-3a regulates somite and tailbud formation in the mouse embryo. *Genes Dev.* **8**, 174–189 (1994). doi: [10.1101/gad.8.2.174](https://doi.org/10.1101/gad.8.2.174); pmid: 8299937
11. T. P. Yamaguchi, K. Harpal, M. Henkemeyer, J. Rossant, fgfr-1 is required for embryonic growth and mesodermal patterning during mouse gastrulation. *Genes Dev.* **8**, 3032–3044 (1994). doi: [10.1101/gad.8.24.3032](https://doi.org/10.1101/gad.8.24.3032); pmid: 8001822
12. A. Iulianella, B. Beckett, M. Petkovich, D. Lohnes, A molecular basis for retinoic acid-induced axial truncation. *Dev. Biol.* **205**, 33–48 (1999). doi: [10.1006/dbio.1998.9110](https://doi.org/10.1006/dbio.1998.9110); pmid: 9882496
13. T. Yoshino, H. Murai, D. Saito, Hedgehog-BMP signalling establishes dorsoventral patterning in lateral plate mesoderm to trigger gonadogenesis in chicken embryos. *Nat. Commun.* **7**, 12561 (2016). doi: [10.1038/ncomms12561](https://doi.org/10.1038/ncomms12561); pmid: 27558761
14. Y. C. Hu, L. M. Okumura, D. C. Page, Gata4 is required for formation of the genital ridge in mice. *PLoS Genet.* **9**, e1003629 (2013). doi: [10.1371/journal.pgen.1003629](https://doi.org/10.1371/journal.pgen.1003629); pmid: 23874227
15. D. Wilhelm, C. Englert, The Wilms tumor suppressor WT1 regulates early gonad development by activation of Sf1. *Genes Dev.* **16**, 1839–1851 (2002). doi: [10.1101/gad.220102](https://doi.org/10.1101/gad.220102); pmid: 12130543
16. M. Chen *et al.*, Wt1 directs the lineage specification of sertoli and granulosa cells by repressing Sf1 expression. *Development* **144**, 44–53 (2017). pmid: 27888191
17. X. Luo, Y. Ikeda, K. L. Parker, A cell-specific nuclear receptor is essential for adrenal and gonadal development and sexual differentiation. *Cell* **77**, 481–490 (1994). doi: [10.1016/0092-8674\(94\)90211-9](https://doi.org/10.1016/0092-8674(94)90211-9); pmid: 8187173
18. M. Kusaka *et al.*, Abnormal epithelial cell polarity and ectopic epidermal growth factor receptor (EGFR) expression induced in Emx2 KO embryonic gonads. *Endocrinology* **151**, 5893–5904 (2010). doi: [10.1210/en.2010-0915](https://doi.org/10.1210/en.2010-0915); pmid: 20962046
19. S. Kuroki *et al.*, Epigenetic regulation of mouse sex determination by the histone demethylase Jmjd1a. *Science* **341**, 1106–1109 (2013). doi: [10.1126/science.1239864](https://doi.org/10.1126/science.1239864); pmid: 24009392
20. D. Schmidt *et al.*, The murine winged-helix transcription factor Foxl2 is required for granulosa cell differentiation and ovary maintenance. *Development* **131**, 933–942 (2004). doi: [10.1242/dev.00969](https://doi.org/10.1242/dev.00969); pmid: 14736745
21. A. Auguste *et al.*, Loss of R-spondin1 and Foxl2 amplifies female-to-male sex reversal in XX mice. *Sex Dev.* **5**, 304–317 (2011). doi: [10.1159/000334517](https://doi.org/10.1159/000334517); pmid: 22116255
22. S. E. Gustin *et al.*, WNT/ β -catenin and p27/FOXL2 differentially regulate supporting cell proliferation in the developing ovary. *Dev. Biol.* **412**, 250–260 (2016). doi: [10.1016/j.ydbio.2016.02.024](https://doi.org/10.1016/j.ydbio.2016.02.024); pmid: 26939755
23. M. C. Nostro, X. Cheng, G. M. Keller, P. Gadue, Wnt, activin, and BMP signaling regulate distinct stages in the developmental pathway from embryonic stem cells to blood. *Cell Stem Cell* **2**, 60–71 (2008). doi: [10.1016/j.stem.2007.10.011](https://doi.org/10.1016/j.stem.2007.10.011); pmid: 18371422
24. Y. Sasagawa *et al.*, Quartz-Seq: A highly reproducible and sensitive single-cell RNA sequencing method, reveals non-genetic gene-expression heterogeneity. *Genome Biol.* **14**, R31 (2013). doi: [10.1186/gb-2013-14-4-r31](https://doi.org/10.1186/gb-2013-14-4-r31); pmid: 23594475
25. F. Buettner *et al.*, Computational analysis of cell-to-cell heterogeneity in single-cell RNA-sequencing data reveals hidden subpopulations of cells. *Nat. Biotechnol.* **33**, 155–160 (2015). doi: [10.1038/nbt.3102](https://doi.org/10.1038/nbt.3102); pmid: 25599176
26. L. Mork *et al.*, Temporal differences in granulosa cell specification in the ovary reflect distinct follicle fates in mice. *Biol. Reprod.* **86**, 37 (2012). doi: [10.1095/biolreprod.111.095208](https://doi.org/10.1095/biolreprod.111.095208); pmid: 21976597
27. Y. Morita-Fujimura, Y. Tokitake, Y. Matsui, Heterogeneity of mouse primordial germ cells reflecting the distinct status of their differentiation, proliferation and apoptosis can be classified by the expression of cell surface proteins integrin $\alpha 6$ and c-Kit. *Dev. Growth Differ.* **51**, 567–583 (2009). doi: [10.1111/j.1440-169X.2009.01119.x](https://doi.org/10.1111/j.1440-169X.2009.01119.x); pmid: 21314674
28. N. Hamada *et al.*, Germ cell-intrinsic effects of sex chromosomes on early oocyte differentiation in mice. *PLoS Genet.* **16**, e1008676 (2020). doi: [10.1371/journal.pgen.1008676](https://doi.org/10.1371/journal.pgen.1008676); pmid: 32214314
29. K. Takasawa *et al.*, FOXL2 transcriptionally represses Sf1 expression by antagonizing WT1 during ovarian development in mice. *FASEB J.* **28**, 2020–2028 (2014). doi: [10.1096/fj.13-246108](https://doi.org/10.1096/fj.13-246108); pmid: 24451388
30. K. Miyabayashi *et al.*, Heterogeneity of ovarian theca and interstitial gland cells in mice. *PLoS ONE* **10**, e0128352 (2015). doi: [10.1371/journal.pone.0128352](https://doi.org/10.1371/journal.pone.0128352); pmid: 26039146
31. R. Li, D. F. Albertini, The road to maturation: Somatic cell interaction and self-organization of the mammalian oocyte. *Nat. Rev. Mol. Cell Biol.* **14**, 141–152 (2013). doi: [10.1038/nrm3531](https://doi.org/10.1038/nrm3531); pmid: 23429793
32. K. Hayashi, O. Hikabe, Y. Obata, Y. Hirao, Reconstitution of mouse oogenesis in a dish from pluripotent stem cells. *Nat. Protoc.* **12**, 1733–1744 (2017). doi: [10.1038/nprot.2017.070](https://doi.org/10.1038/nprot.2017.070); pmid: 28796232
33. N. Hamazaki *et al.*, Reconstitution of the oocyte transcriptional network with transcription factors. *Nature* **589**, 264–269 (2021). doi: [10.1038/s41586-020-3027-9](https://doi.org/10.1038/s41586-020-3027-9); pmid: 33328630
34. T. Furusawa, K. Ohkoshi, C. Honda, S. Takahashi, T. Tokunaga, Embryonic stem cells expressing both platelet endothelial cell adhesion molecule-1 and stage-specific embryonic antigen-1 differentiate predominantly into epiblast cells in a chimeric embryo. *Biol. Reprod.* **70**, 1452–1457 (2004). doi: [10.1095/biolreprod.103.024190](https://doi.org/10.1095/biolreprod.103.024190); pmid: 14736812
35. M. S. Kowalczyk *et al.*, Single-cell RNA-seq reveals changes in cell cycle and differentiation programs upon aging of hematopoietic stem cells. *Genome Res.* **25**, 1860–1872 (2015). doi: [10.1101/gr.192237.115](https://doi.org/10.1101/gr.192237.115); pmid: 26430063
36. Data for: T. Yoshino *et al.*, Generation of ovarian follicles from mouse pluripotent stem cells. *Zenodo* (2021); <https://doi.org/10.5281/zenodo.4775540>.

ACKNOWLEDGMENTS

We thank F. Arai for technical support, H. Sasaki for providing T-GFP mice, B. Roelen and S. M. C. de Sousa Lopes for comments on the manuscript, and the Research Support Center, Kyushu University Graduate School of Medical Sciences, for technical assistance. **Funding:** This work was supported in part by KAKENHI Grants-in-Aid from MEXT, Japan (nos. 17H01395, 18H05544, and 18H05545 to K.H.; nos. 19K06678 and 20H04926 to T.Y.; no. 17H06177 to R.N.; nos. 17H06427 and 20H03436 to K.M.; no. 19K07378 to Y.S.; and no. 17H06424 to M.T.); by the Takeda Science Foundation (K.H.); by the Luca Bella Foundation (K.H.); and by a Grant-in-Aid from The Open Philanthropy Project, Silicon Valley Community Foundation (K.H.). **Author contributions:** T.Y. and K.H. conceived and designed the project. T.Y., G.N., H.K., and K.H. performed the cellular and embryonic experiments. T.S., H.Y., M.I., M.K., T.I., and K.N. performed single-cell sequencing analysis. R.N., M.T., G.N., M.I., Y.S., and K.M. provided materials. K.H. and T.Y. wrote the manuscript, incorporating feedback from all the authors. **Competing interests:** The authors declare no competing financial interests. **Data and materials availability:** The RNA-sequencing data have been deposited at the Gene Expression Omnibus (GEO) database under accession number GSE151143. R scripts generated for the analysis are available on GitHub (<https://github.com/takahirosuzuki0626/FOSLCs>) and Zenodo (36). All materials are available from the corresponding authors upon request.

SUPPLEMENTARY MATERIALS

science.sciencemag.org/content/373/6552/eabe0237/suppl/DC1
Materials and Methods
Figs. S1 to S11
Tables S1 to S6
References (37–43)
MDAR Reproducibility Checklist

[View/request a protocol for this paper from Bio-protocol.](#)

27 July 2020; accepted 28 May 2021
10.1126/science.abe0237

Generation of ovarian follicles from mouse pluripotent stem cells

Takashi Yoshino, Takahiro Suzuki, Go Nagamatsu, Haruka Yabukami, Mika Ikegaya, Mami Kishima, Haruka Kita, Takuya Imamura, Kinichi Nakashima, Ryuichi Nishinakamura, Makoto Tachibana, Miki Inoue, Yuichi Shima, Ken-ichirou Morohashi and Katsuhiko Hayashi

Science **373** (6552), eabe0237.
DOI: 10.1126/science.abe0237

Reconstituting the ovarian follicle

Recent advances have enabled the generation of oocytes from pluripotent stem cells in vitro. However, these cells require a somatic environment to develop fully as reproductive cells. Yoshino *et al.* applied what is known about differentiation processes in vivo to determine a culture condition to differentiate embryonic stem cells into gonadal somatic cell–like cells (see the Perspective by Yang and Ng). When the embryonic stem cell–generated ovarian gonadal tissue was combined with early primordial germ cells or in vitro–derived primordial germ cell–like cells, germ cells developed into viable oocytes within the reconstituted follicles that could be fertilized and result in viable offspring. This system enables an alternative method for mouse gamete production and advances our understanding of mammalian reproduction and development.

Science, eabe0237, this issue p. eabe0237; see also abj8347, p. 282

ARTICLE TOOLS

<http://science.sciencemag.org/content/373/6552/eabe0237>

SUPPLEMENTARY MATERIALS

<http://science.sciencemag.org/content/suppl/2021/07/14/373.6552.eabe0237.DC1>

RELATED CONTENT

<http://science.sciencemag.org/content/sci/373/6552/282.full>

REFERENCES

This article cites 42 articles, 10 of which you can access for free
<http://science.sciencemag.org/content/373/6552/eabe0237#BIBL>

PERMISSIONS

<http://www.sciencemag.org/help/reprints-and-permissions>

Use of this article is subject to the [Terms of Service](#)

Science (print ISSN 0036-8075; online ISSN 1095-9203) is published by the American Association for the Advancement of Science, 1200 New York Avenue NW, Washington, DC 20005. The title *Science* is a registered trademark of AAAS.

Copyright © 2021 The Authors, some rights reserved; exclusive licensee American Association for the Advancement of Science. No claim to original U.S. Government Works